Hot-Wire Measurements of Statistical and Spectral Evolution of an Axisymmetric Turbulent Jet

by

Kevin Daniel Galli

Submitted to the Department of Mechanical Engineering
in partial fulfillment of the requirements for the degree of

Bachelor of Science

at the

MASSACHUSETTS INSTITUTE OF TECHNOLOGY

June 1991

Author .....
Department of Mechanical Engineering
May 10, 1991

Certified by .....
John H. Lienhard V
Assistant Professor of Mechanical Engineering
Thesis Supervisor

Accepted by .....
Peter Griffith
Chairman, Departmental Committee

Hot-Wire Measurements of Statistical and Spectral Evolution of an Axisymmetric Turbulent Jet

by

Kevin Daniel Galli

Submitted to the Department of Mechanical Engineering
on May 10, 1991, in partial fulfillment of the
requirements for the degree of
Bachelor of Science

Abstract

Velocity measurements of an axisymmetric turbulent jet were made using a hot-wire anemometer. The jet was a round free gas jet with a nozzle of $D_o = 3.18$ mm diameter. The non-dimensional axial mean velocity distribution was obtained for jets with Reynolds numbers from 10,000 to 26,540. The non-dimensional axial rms velocity distribution and the relative turbulence intensities were obtained for Reynolds numbers from 10,000 to 27,900. The power spectra of the jet at a Reynolds number of 20,000 were obtained by performing fast Fourier transforms on the square of the turbulent velocity signal.

The velocity measurements were compared to those obtained by Simo (1991) and to the theoretical predictions of Hinze (1975). The axial mean and rms velocity distributions showed good qualitative agreement to Simo's results and Hinze's prediction for all Reynolds numbers downstream distances of $x/D_o > 15$, although the results were quantitatively between 10% and 50% lower than the earlier results. The turbulence intensities varied widely from Hinze's theoretical prediction and Simo's results, due to white noise in the velocity measurement sytem. The power spectra of the jet at Reynolds number 20,000 show the expected decrease in density as the frequency increases. The white noise present in the turbulent velocity signal can be observed in the power spectra as they fall off at high frequecies.

The best correlation between the experimental and theoretical results for the axial velocity distributions was for Reynolds numbers of 20,000 or more, suggesting that there may be a lower bound for which Hinze's prediction for centerline velocity is applicable.

Thesis Supervisor: John H. Lienhard V
Title: Assistant Professor of Mechanical Engineering

Acknowledgments

I would like to thank my parents, Daniel J. and Ellen M. Galli, for all the love and support which they have given me throughout my academic career.

Special thanks to Professor John H. Lienhard V, without whose guidance, patience and understanding this thesis would never have been completed.

I would also like to thank all of my friends from East Campus, the Mechanical Engineering Department, and the MIT mens' soccer team for their friendship and support which has helped keep me sane for the last four years.

Thanks to Kristin for being there to put a smile on my face.

"Once in a while you get shown the light, in the strangest of places, if you look at it right."

-Hunter/Garcia, *Scarlet Begonias*

Contents

List of Figures

Chapter 1

Introduction

A jet may be generally defined as a high-velocity stream of fluid which emanates under pressure from a small-diameter opening or nozzle. The term turbulent implies that the flow within the jet is characterized by random fluctuations in fluid velocity. The study of the fluid motion of turbulent jets has many real-world applications, among which are the fuel injectors of automobile engines, and the particle dispersion of aerosols.

My purpose is to confirm, using a hot-wire anemometer, various velocity measurements of an axisymmetric turbulent jet made by Simo (1991), using a laser doppler velocity measurement system. Of particular interest are the axial mean and rms velocity distributions and the relative intensity of the turbulent velocity fluctuations.

A turbulent flow is an irregular flow characterized by random fluctuations in fluid velocity with time and space coordinates, and intense mixing of the fluid on the macroscopic level. For a steady turbulent flow, a statistical time-average velocity may be discerned. The turbulent flow of a round free jet is axisymmetrical in nature; that is, the turbulence is statistically symmetric about the axis of the flow direction. For this reason, it is primarily of interest to consider the fluid velocity at various points along the centerline of the jet. In order to define the downstream distance for which turbulent velocity measurements are of interest, the axial mean velocity distribution was determined for various Reynolds numbers and compared to Hinze's theoretical prediction.

The relative intensity of the fluctuations in velocity due to the effect of turbulence was also examined. In order to do this, the hot-wire anemometer was AC-coupled in order that the root-mean square (rms) value of the velocity fluctuation about the average value could be determined. The axial distribution of the rms velocity was determined, as for the mean velocity. The relative intensity of the fluctuation as compared to the average velocity of the jet was then plotted against the relative downstream distance.

Finally, it is of interest to obtain the power spectra of the turbulent velocity fluctuations, in order to find which frequencies of the turbulent velocity signal carry the most energy. This was accomplished by performing a Fourier transform on the square of the turbulent velocity signal at various downstream distances for a particular Reynolds number.

Chapter 2 outlines the theoretical predictions for turbulent jet velocities. Chapter 3 provides a description of the equipment used in the experiments and the calibration procedure for the hot-wire anemometer, as well as the procedure for the velocity measurements. Chapter 4 contains the results of the experiments for various Reynolds numbers ranging from 10,000 to 27,900. The remaining chapters compare the experimental results to those predicted by theory and to those experimentally obtained by Simo.

Chapter 2

Theoretical Analysis

For a round free jet, the Reynolds number R_e is defined as:

$$R_e \equiv \frac{U_o D_o}{\nu} \tag{2.1}$$

where U_o is the exit velocity of the jet, D_o is the diameter of the jet nozzle, and ν is the kinematic viscosity of the fluid. Physically, this dimensionless parameter is an estimate of the inertia force of the flow over the viscous force.[1] In general, a flow will be turbulent for a large Reynolds number of 10^4 or greater. Since in this case the kinematic viscosity of air is constant, and the exit diameter of the nozzle was also constant, the Reynolds number of the flow can be varied by changing the exit velocity of the jet.

The axial velocity of a turbulent jet is a function of the Reynolds number as well as the downstream distance. A typical axisymmetric turbulent jet is shown in Figure 2-1 in order to define the quantities which are relevant in velocity measurements. The jet has a nozzle diameter of D_o, an exit velocity of U_o, and is statistically symmetric about the x axis.

In making measurements of the velocity of a turbulent jet, consideration is first given to the axial mean velocity distribution. Hinze (1975) gave a relation for the centerline mean velocity in a round free gas-phase jet:

[1] Gerhart 379.

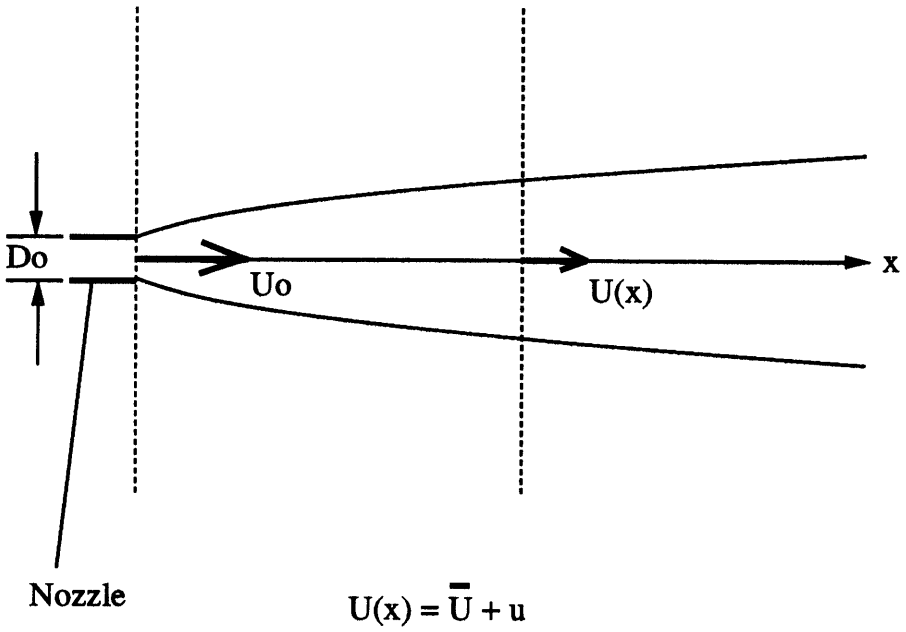

Figure 2-1: An Axisymmetric Turbulent Jet.

$$\frac{U}{U_o} = \frac{5.9}{\frac{x}{D_o - 0.5}} \tag{2.2}$$

After the mean velocity distribution has been determined, the turbulent velocity fluctuations should be considered. Of particular interest is the relative intensity of the fluctuations compared to the mean velocity.

At any given time t, the momentary value of the velocity of the fluid in the turbulent jet, U, may be expressed as:

$$U = \bar{U} + u \tag{2.3}$$

where $\bar{U}$ represents the average value of the velocity, and u is the value of the fluctuation. Because the mean value of the fluctuations will be zero, the intensity of the turbulence fluctuations is usually expressed by the root mean square (rms) value

$$u' = \sqrt{\bar{u^2}} \tag{2.4}$$

The relative intensity of the fluctuations is then given by the ratio $u'/\bar{U}$. The average velocity $\bar{U}$ is the time-average of the velocity at a point along the axis of the jet.

Along the centerline of a round free jet, the rms velocity fluctuations are related to the mean velocity as:

$$u' = 0.25U \tag{2.5}$$

Substituting this expression into Equation 2.2, we obtain the following relation for the axial rms velocity distribution:

$$\frac{u'}{U_o} = \frac{1.5}{\frac{x}{D_o - 0.5}} \tag{2.6}$$

In order to obtain the power spectra of the jet, a Fourier transform must be performed on the square of the turbulent velocity waveform. Fourier analysis is dependent on the fact that a periodic or aperiodic function may be expressed as the

sum of waveforms of different frequencies. An aperiodic function such as the turbulent velocity waveform may be expressed as

$$x(t) = \sum C_n e^{i2\pi nt/T} \tag{2.7}$$

The frequency spectrum of such a function can be found by a discrete Fourier transform,

$$X_k = \frac{1}{N} \sum x(r) e^{-i2\pi nt/T} \tag{2.8}$$

A fast Fourier transform chooses N as a power of 2 in order to reduce the number of mathematical operations necessary to obtain the frequency spectrum.

The correlation $u(t)u(\bar{t}+\tau)$ is called the autocorrelation between the values of u at two different times. The power spectrum $S_{uu}(f)$ is the Fourier transform of this correlation:

$$S_{uu}(f) = \int u(t)u(\bar{t}+\tau)e^{i2\pi f\tau} d\tau \tag{2.9}$$

The power spectrum represents the mean-square amplitude of the turbulent velocity signal. It may be thought of as the energy in $u(t)$ at a particular frequency.[2] By plotting the power spectra of the jet at various downstream distances, it is possible to discern which frequencies carry the most energy.

[2]Tennekes 210-215.

Chapter 3

Experimental Apparatus and Procedure

3.1 Overview of Apparatus

The apparatus used for the velocity measurements is shown in Figure 3-1. This apparatus consisted of a house compressed air supply with a pressure regulator, a nozzle to produce the jet, the hot-wire anemometer, a TSI bridge, a dual-track voltage supply, an oscilloscope, a digital multimeter, and a voltmeter and personal computer for data acquisition. A Pitot tube and a manometer were also used, in order to calibrate the hot-wire anemometer. The only physical dimension of the experimental apparatus which is of consequence in analysis is the diameter D_o of the jet nozzle, which was 3.18 mm.

The pressure regulator was used to control the exit velocity of the turbulent air jet. The hot-wire anemometer was placed downstream at various points along the axis of the jet. The probe was connected to the TSI bridge, which was powered by the dual track voltage supply. The output voltage from the bridge was sent to the oscilloscope and digital multimeter so that it could be recorded. The scope was AC-coupled for the rms velocity measurements. For the power spectra measurements, the output voltage of the probe was filtered to remove its DC component. Then the waveform of the turbulent velocity fluctuation was captured and a fast Fourier transform was

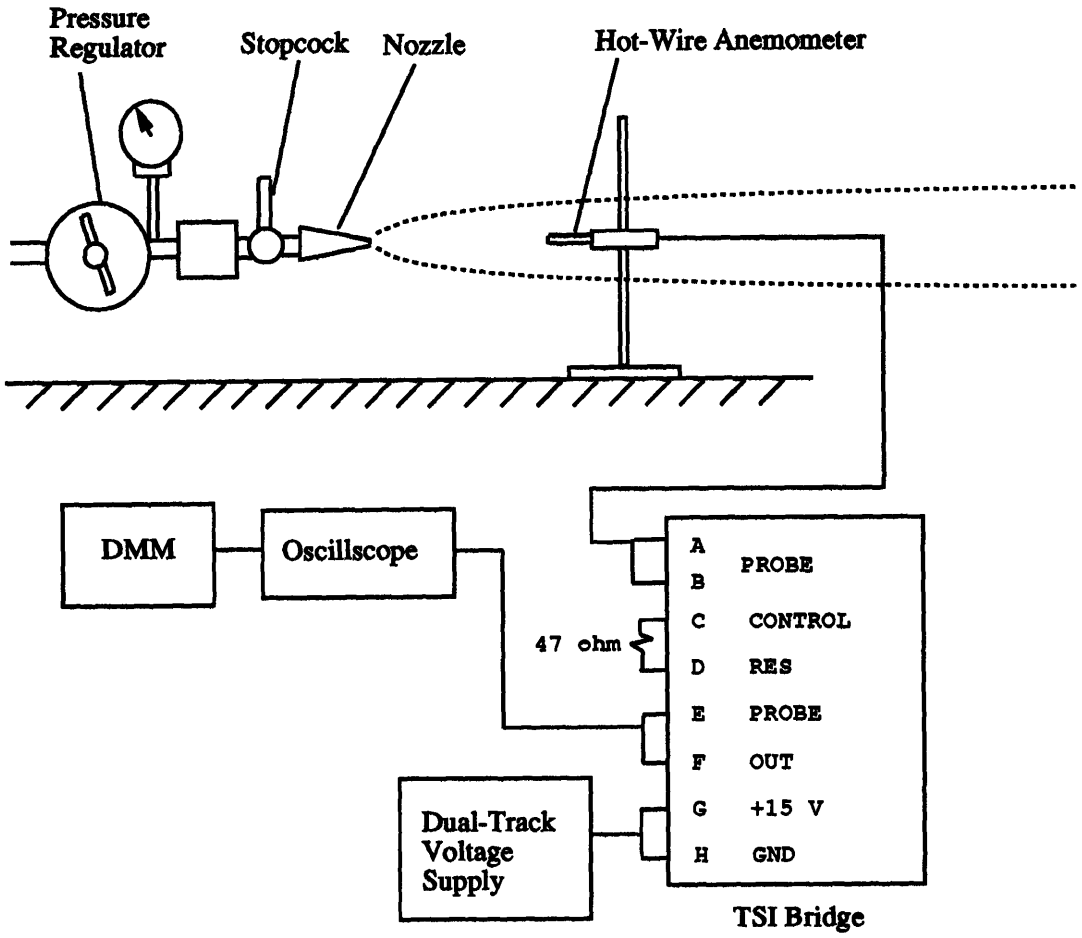

Figure 3-1: Experimental Apparatus.

performed using the computer.

3.2 The Hot-Wire Anemometer

The hot-wire anemometer was used in the velocity measurements because it is an excellent instrument for measuring turbulent flow. Its small size causes only a minimal disturbance of the flow pattern, and its high frequency response and sensitivity allow the hot-wire probe to capture the turbulent velocity fluctuations which are of interest.

The hot-wire anemometer uses a very fine, short metal wire as the detecting element. The wire is cooled by the flowing fluid through heat conduction, free and forced convection, and radiation. The drop in the wire's temperature causes the electrical resistance of the wire to decrease. By using the hot-wire probe in a Wheatstone bridge circuit with feedback, the electrical resistance of the wire can be held constant. Consequently, the temperature of the wire will also be held constant. The fluctuating electric current which is required to hold the wire temperature constant is read as a voltage. From the output voltage, the velocity of the flow is determined.

In high Reynolds number flow, the heat transfer effects of conduction, free convection and radiation are negligible compared to those of forced convection. For forced convection, the heat loss Q is given as:

$$Q = hA_w(T_w - T_f) = \frac{V_w^2}{R_w} \tag{3.1}$$

where h is the heat transfer coefficient, A_w is the cross-sectional area of the wire, T_w is the temperature of the wire and T_f is that of the fluid.[1] The quantity V_w^2/R_w is the electric power generated in the wire, which is equivalent to the heat loss of the system.

From heat transfer theory, the heat transfer coefficient h is related to the velocity of the fluid as:

[1] Lienhard 16.

$$h = A + BU^{1/2} \tag{3.2}$$

From the voltage divider of the hot-wire bridge, the voltage across the hot-wire anemometer can be expressed as

$$V_w = V_o(\frac{R_w}{R_w + R_1}) \tag{3.3}$$

where V_o is the output voltage from the bridge.

Rewriting Equation 3.1, we find that

$$A + BU^{1/2} = V_o^2 \frac{R_w}{(R_w + R_1)^2 A_w (T_w - T_f)} \tag{3.4}$$

Since the right side of the equation is constant except for V_o, we obtain the expression

$$V_o^2 = C + DU^{1/2} \tag{3.5}$$

The coefficients C and D are not accurately predictable; therefore it is necessary to calibrate the hot-wire anemometer using known values for the velocity U in order to determine the coefficients.

3.3 Calibration Procedure

In order to calibrate the hot-film anemometer, it is necessary to know the average velocity of the jet. The velocity of the jet can be determined by using a Pitot tube and a manometer. The Pitot tube operates on Bernoulli's principle, which states that in steady flow of incompressible fluid the change in kinetic energy between any two positions in space is equal to the work done by pressure and gravity forces. Bernoulli's equation may be expressed as:

$$\frac{v_1^2}{2} + \frac{P_1}{\rho_g} + gh_1 = \frac{v_2^2}{2} + \frac{P_2}{\rho_g} + gh_2 \tag{3.6}$$

where v_1 and v_2 are the fluid velocities at points 1 and 2 in the flow, P_1 and P_2 are the fluid pressures, h_1 and h_2 are the fluid heights, ρ_g is the density of the fluid, which is air, and g is the acceleration of gravity.[2]

This equation may be solved for the fluid velocity at point 1. We assume that point 2 is the stagnation point of the fluid, where $v_2 = 0$. Since there is no difference in height between point 1 and point 2, the gravity terms of the Bernoulli equation cancel. Thus, we can obtain an expression for the fluid velocity in terms of the pressure difference between the point at which the velocity is measured and the stagnation point, where p_2 is equal to atmospheric pressure. Using a reclining manometer, we can measure this pressure difference. The expression for the fluid velocity then becomes:

$$v_1 = U = \sqrt{\frac{2\rho_w g h_w \sin\theta}{\rho_g}} \tag{3.7}$$

where h_w is the difference of water column heights in the manometer measured in the inclined plane, and θ is the angle from the horizontal at which the manometer is inclined. The quantity ρ_w is the density of water.

From this equation it can be seen that the fluid velocity is proportional to $\sqrt{h_w}$. Since the velocity is also proportional to the output voltage of the hot-wire anemometer, as $\sqrt{U} \propto V_o^2$, it follows that V_o^2 is directly proportional to $h_w^{1/4}$. Thus, to calibrate the hot-wire anemometer, the Pitot probe and manometer are used to determine the fluid velocity at points downstream of the nozzle. Then the hot-wire output voltage at these same points is recorded, and the coefficients C and D of Equation 3.5 are determined by linear regression. As a check that the calibration has been properly performed, a plot of V_o^2 versus $h_w^{1/4}$ is made for the downstream fluid velocities. Since these quantities are directly proportional, a good calibration should produce a linear plot of output voltage versus manometer height.

[2]Gerhart 184-186.

3.4 Experimental Procedure

After the hot-wire probe was calibrated, the velocity measurements were performed. First, the average velocity of the flow was measured at various points along the axis of the jet for a range of relative downstream distances from $x/D_o = 0$ to $x/D_o = 70$. These measurements were repeated for several Reynolds numbers of the jet.

Next, the hot-wire anemometer was AC-coupled so that the turbulent velocity fluctuations could be measured. The axial rms velocity distribution was obtained, and then the relative intensity of the rms value of the fluctuations was plotted against the relative downstream distance to determine where the turbulence was most prominent in the flow.

Finally, the turbulent velocity waveform was captured using the data acquisition system for eight downstream distances at a Reynolds number of 20,000. Fast Fourier transforms were performed on the square of the turbulent signal in order to obtain the power spectra.

Chapter 4

Results

4.1 Axial Velocity Distributions

The axial mean velocity distribution of the jet for Reynolds numbers of 10,000, 15,000, 20,000, and 26,540 is given in Figure 4-1. The distribution is plotted as nondimensional centerline mean velocity U/U_o versus nondimensional downstream distance x/D_o. For comparative purposes, the theoretical mean velocity distribution given by Hinze in Equation 2.2 is also shown on the graph.

The axial rms velocity distribution of the jet is given in Figure 4-2 for Reynolds numbers of 10,000, 15,000, 20,000, and 27,900. This distribution is plotted as nondimensional axial rms velocity u'/U_o versus nondimensional downstream distance x/D_o. The theoretical rms velocity distribution predicted by Hinze (Equation 2.6) is given for comparison.

4.2 Relative Turbulent Intensity

The relative intensity of the turbulent velocity fluctuations is shown in Figure 4-3. This distribution is given as the relative intensity u'/U versus the nondimensional downstream distance x/D_o. The theoretical prediction given in Equation 2.5 is $u'/U = 0.25$; this is plotted on the graph for comparison.

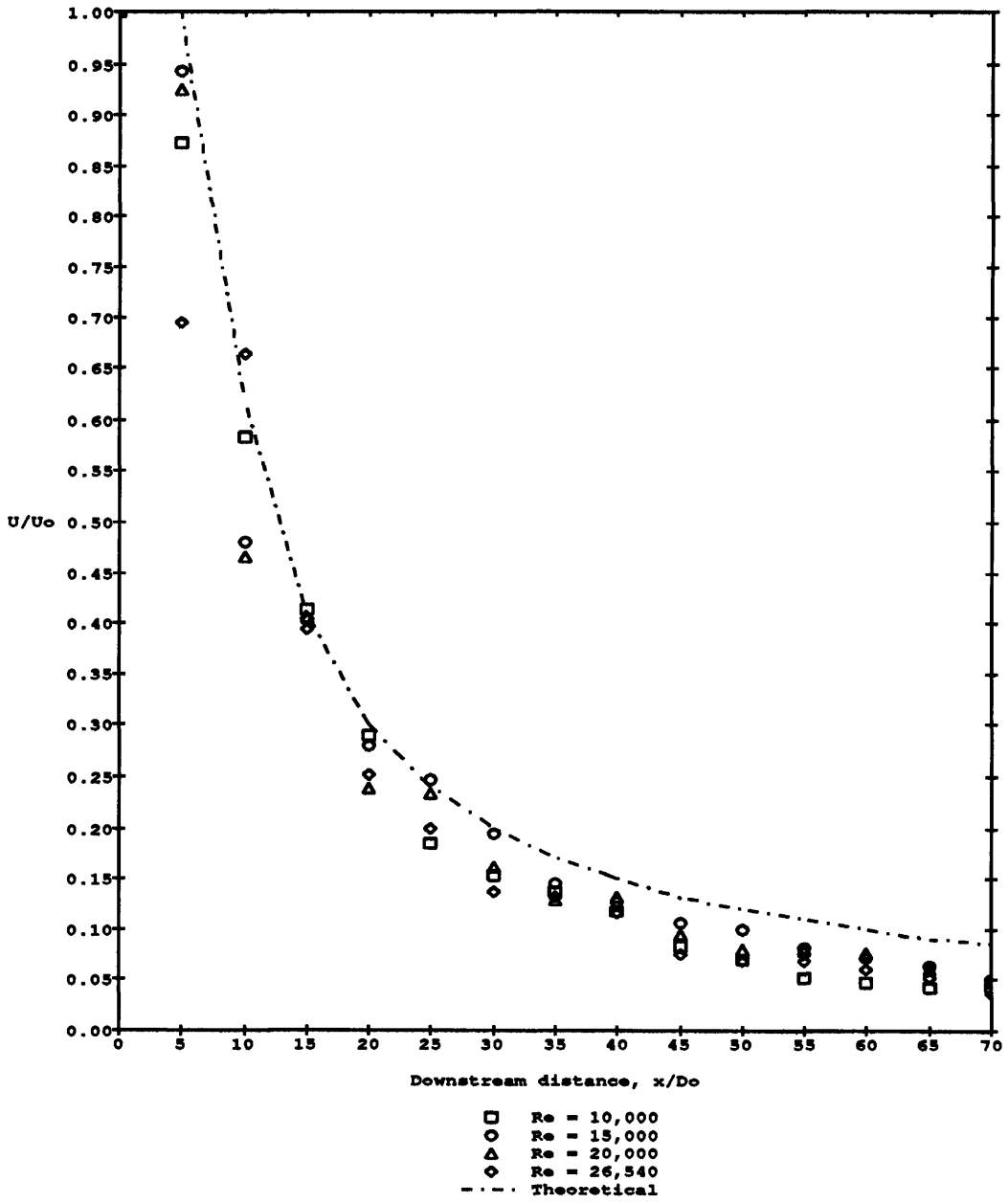

Figure 4-1: Axial Mean Velocity Distribution, U/U_o vs. x/D_o.

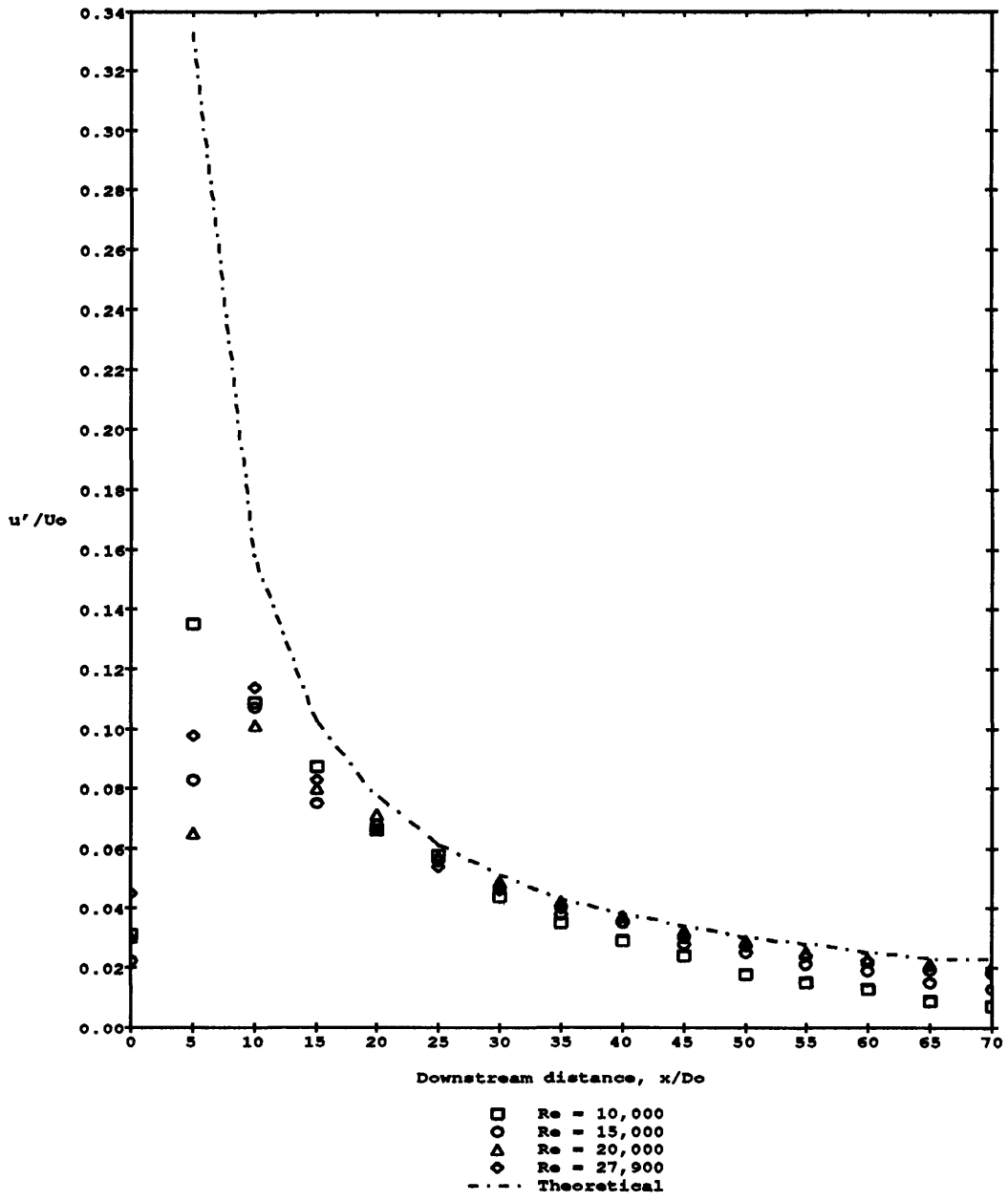

Figure 4-2: Axial RMS Velocity Distribution, u'/U_o vs. x/D_o.

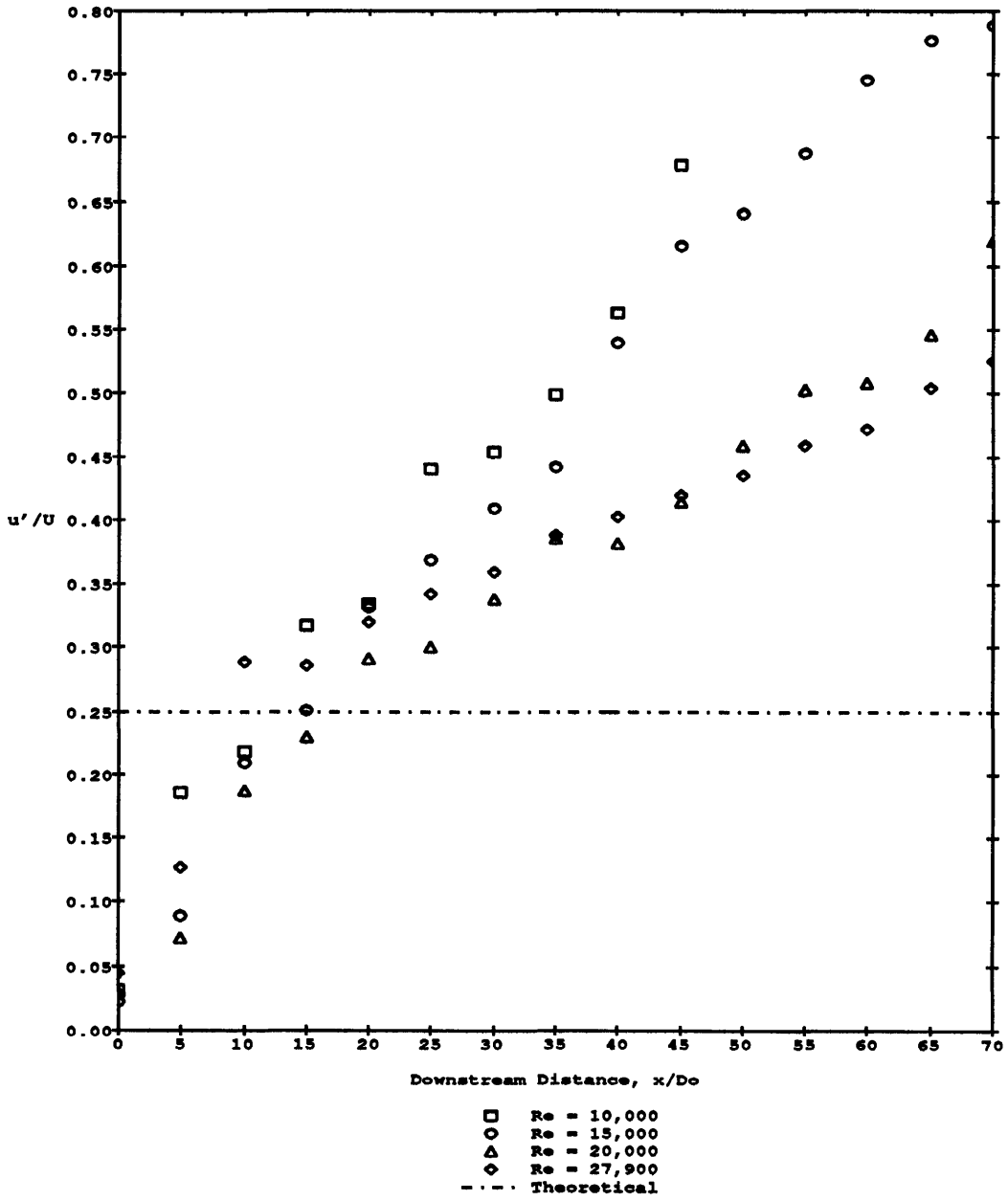

Figure 4-3: Turbulence Intensity u'/U vs. Downstream Distance x/D_o.

4.3 Power Spectra

The turbulent velocity waveform was captured using the data acquisition system for eight downstream distances from $x/D_o = 0$ to $x/D_o = 70$, at a Reynolds number of 20,000. After the waveform was captured, a fast Fourier transform was performed on the square of the data in order to obtain the power spectra of the jet at the various downstream velocities. The power spectra of the jet for $x/D_o = 0$ to $x/D_o = 70$ at $R_e = 20{,}000$ are shown in Figures 4-4 through 4-11.

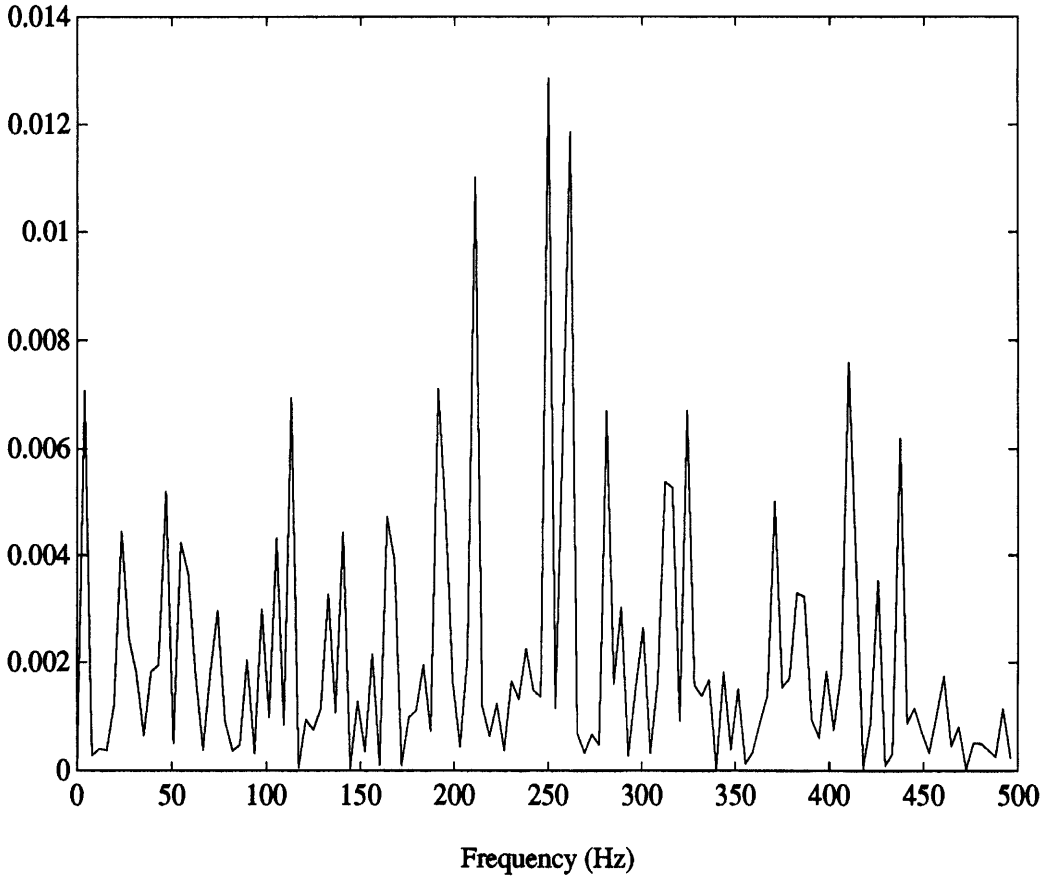

Figure 4-4: Power Spectrum of the Jet Velocity for $x/D_o = 0$.

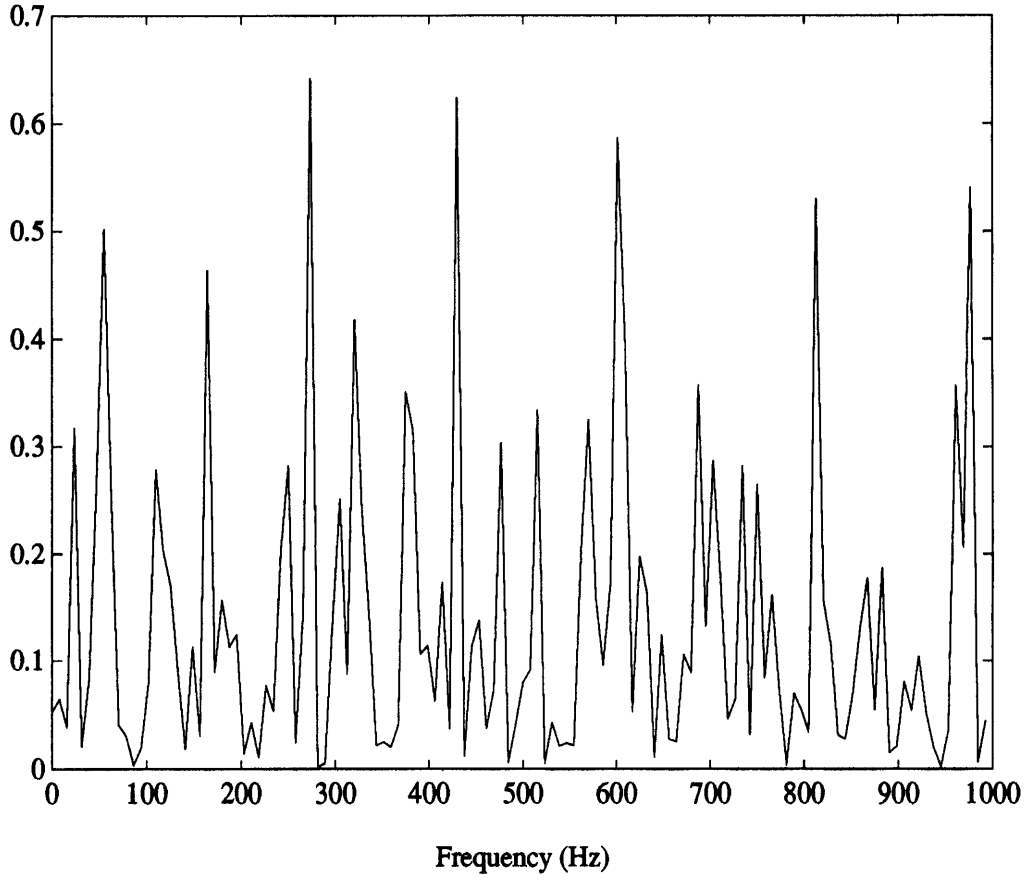

Figure 4-5: Power Spectrum of the Jet Velocity for $x/D_o = 10$.

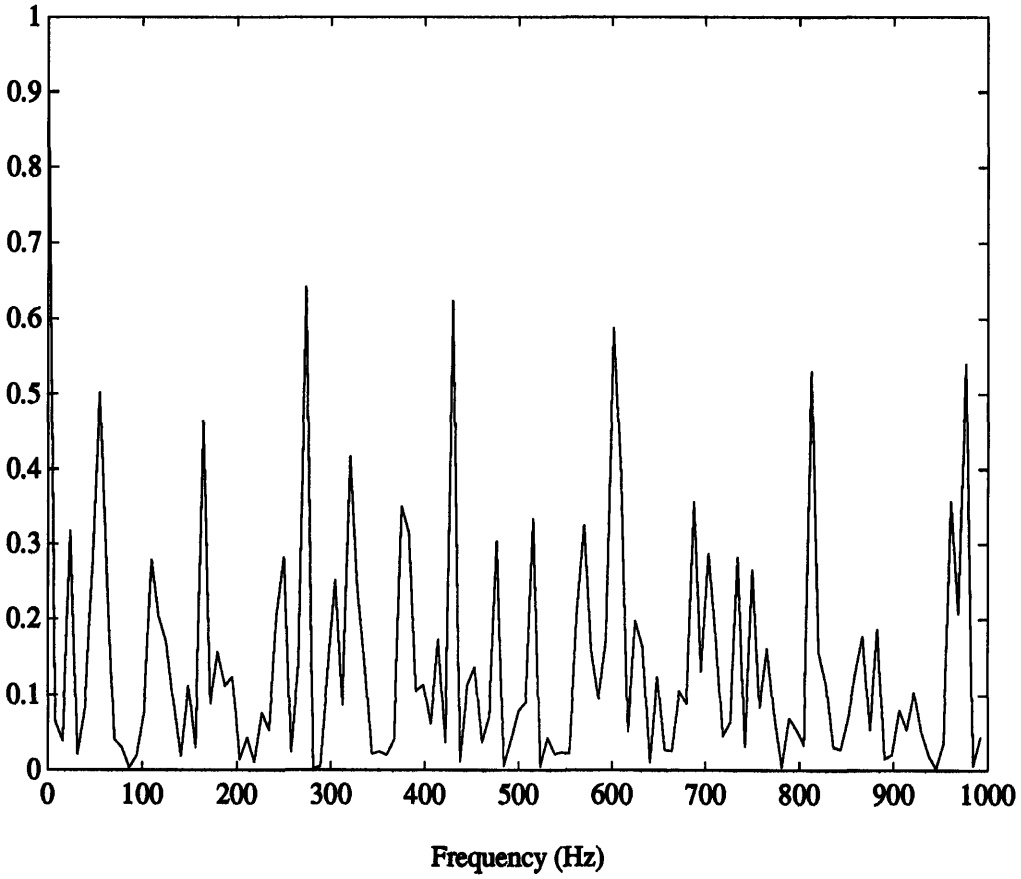

Figure 4-6: Power Spectrum of the Jet Velocity for $x/D_o = 20$.

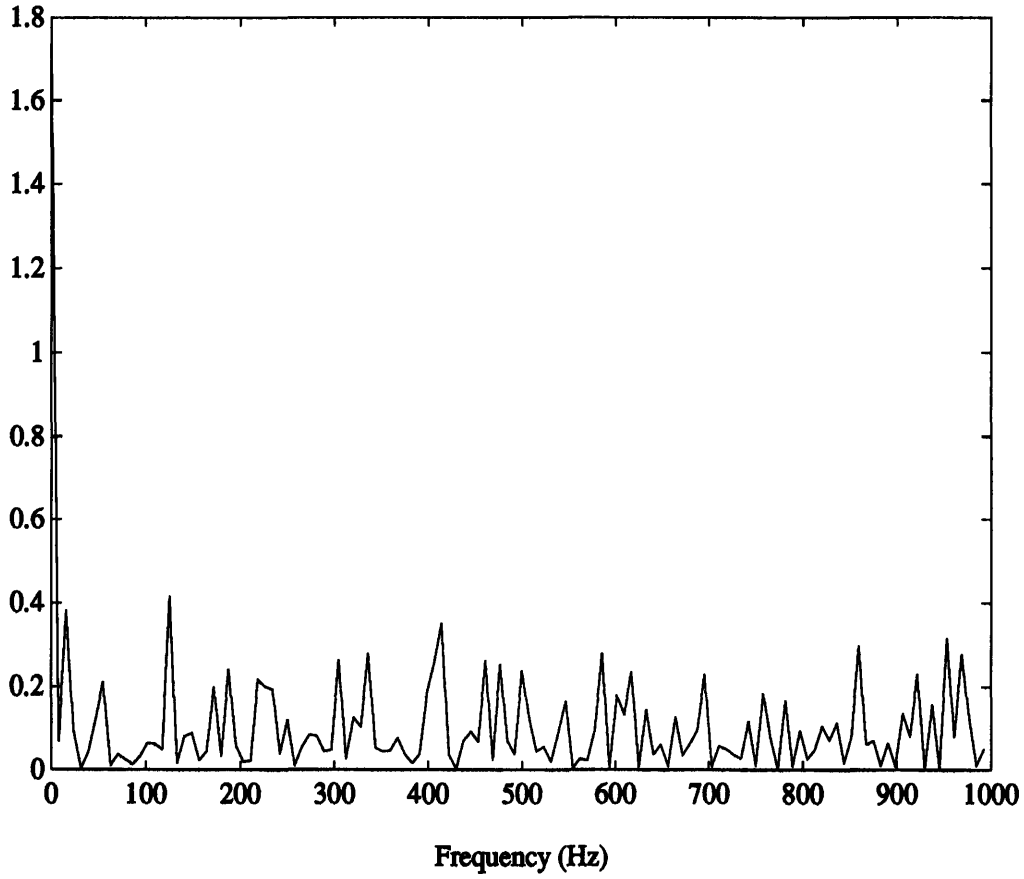

Figure 4-7: Power Spectrum of the Jet Velocity for $x/D_o = 30$.

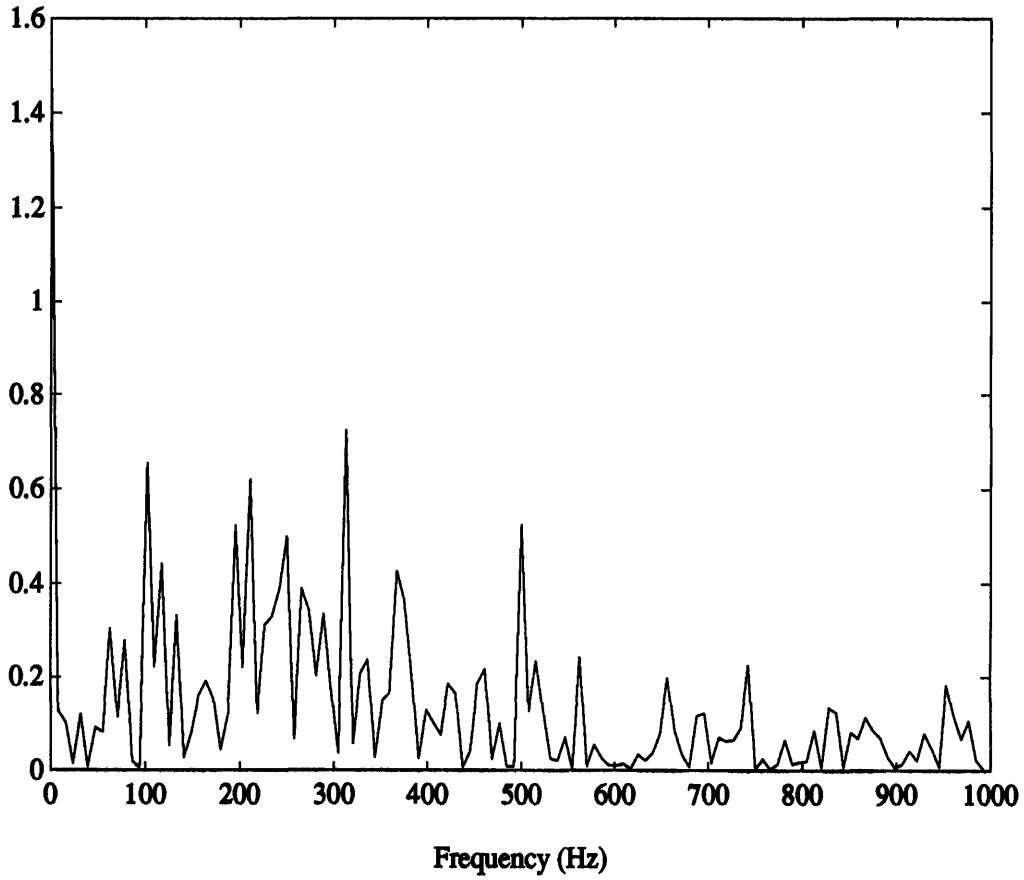

Figure 4-8: Power Spectrum of the Jet Velocity for $x/D_o = 40$.

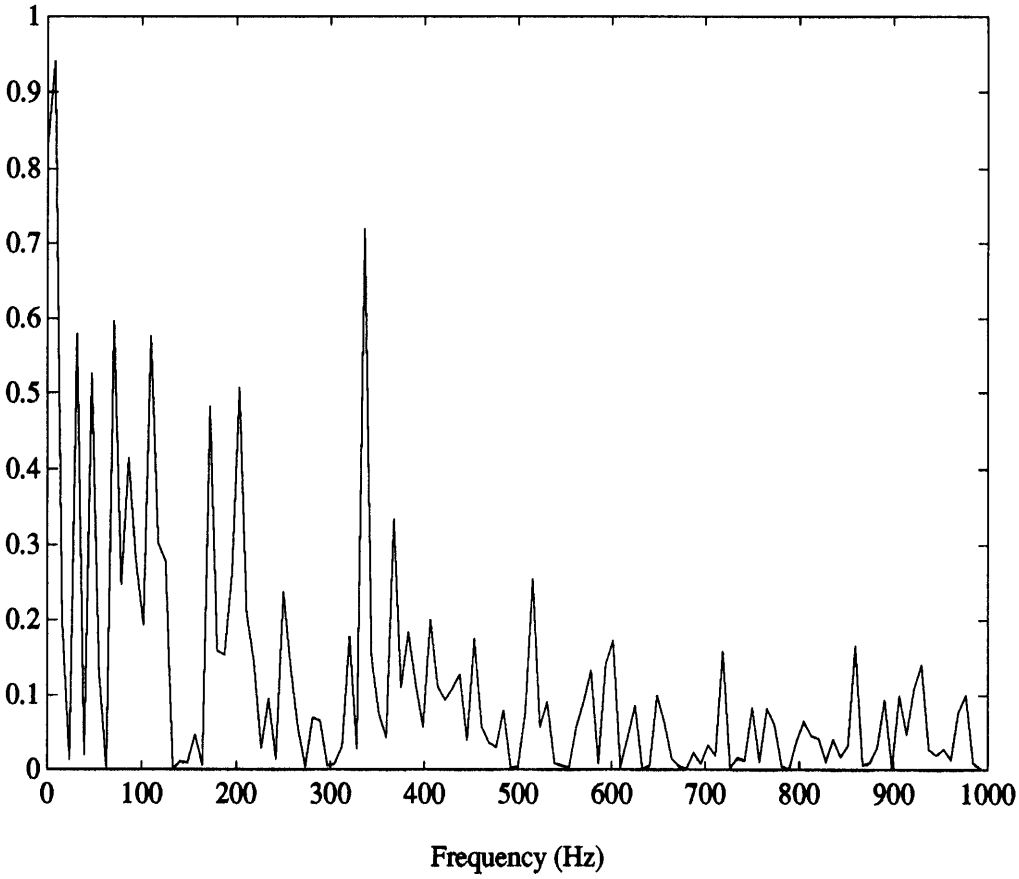

Figure 4-9: Power Spectrum of the Jet Velocity for $x/D_o = 50$.

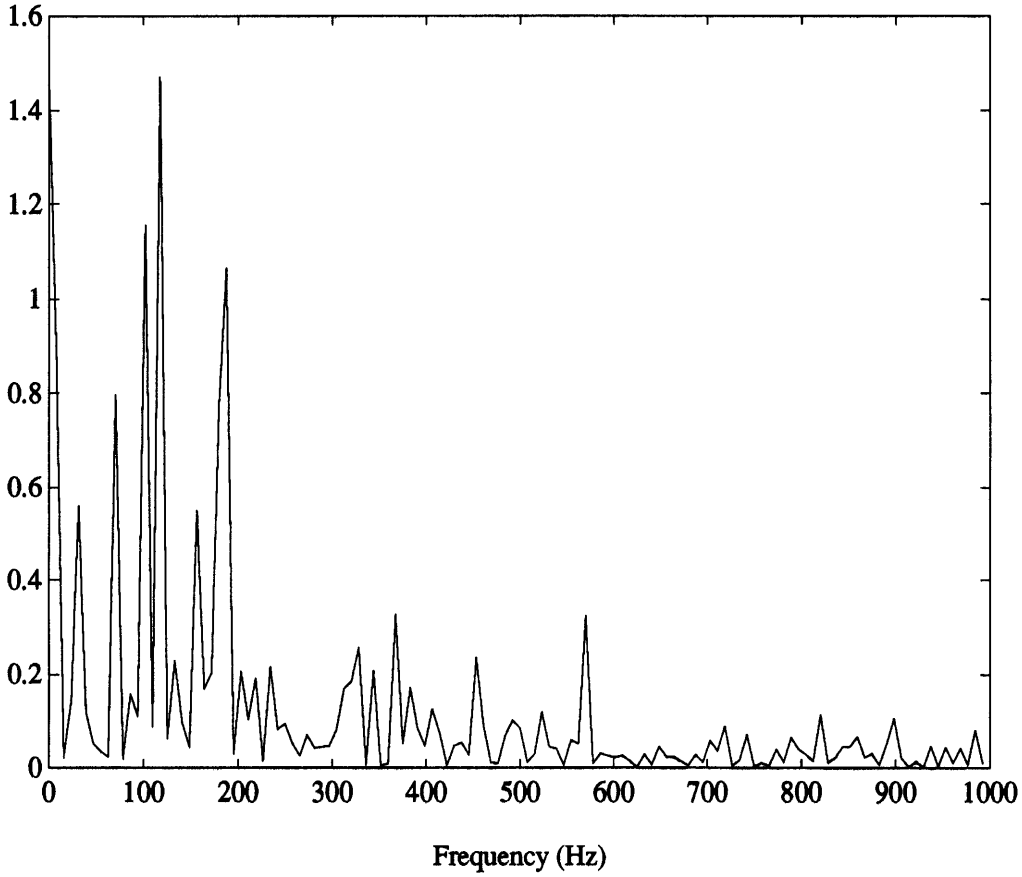

Figure 4-10: Power Spectrum of the Jet Velocity for $x/D_o = 60$.

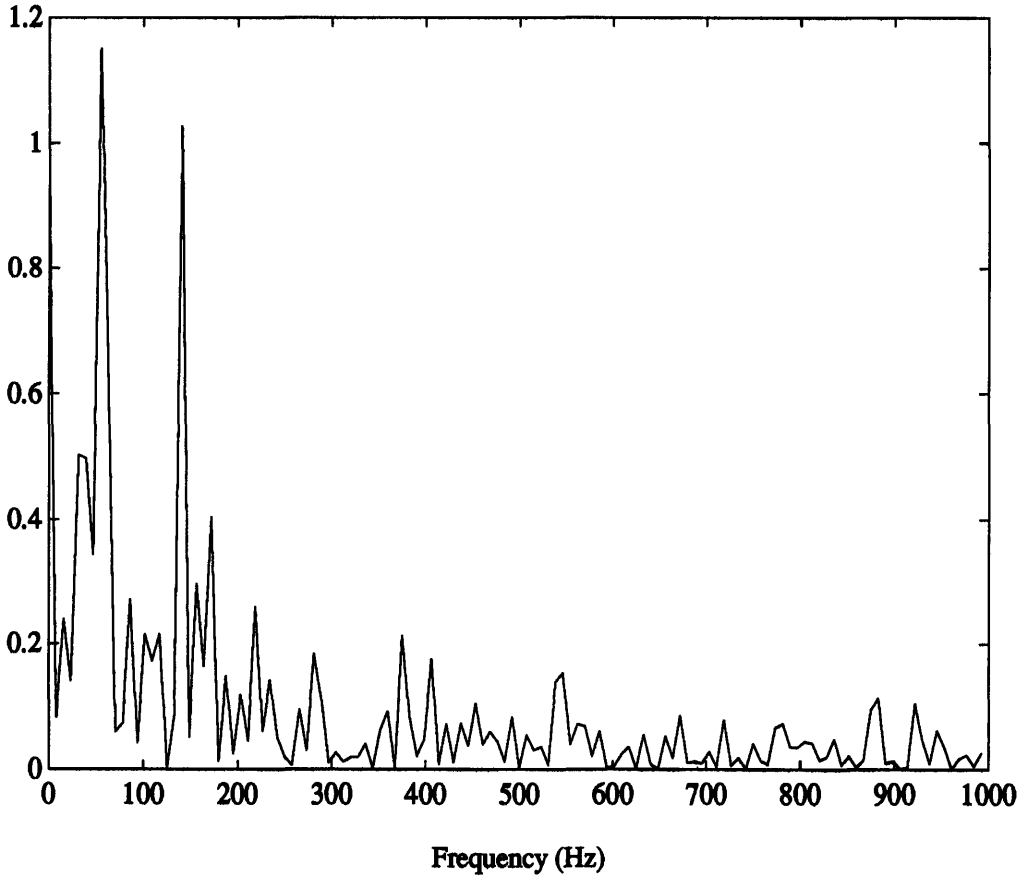

Figure 4-11: Power Spectrum of the Jet Velocity for $x/D_o = 70$.

Chapter 5

Discussion

5.1 Axial Velocity Distributions

The axial mean velocity distribution shown in Figure 4-1 shows good qualitative agreement with the theoretical prediction given by Hinze, especially for downstream distances of $x/D_o > 15$. The shape of the experimental curve for each of the four Reynolds numbers is close to that of the theoretical curve given by Equation 2.2. Quantitatively, the results are almost all lower than the theoretical curve, usually by 0.03 or 0.04 U_o, and have a percentage deviation of between 20% and 50% depending on the downstream distance.

The qualitative agreement between the results and Simo's experimental results is also quite good for most downstream distances, since Simo's results are quite close to the theoretical prediction of Hinze. Since Simo's results lie above the theoretical curve, however, the quantitative disparity is slightly greater. The axial rms velocity distribution shown in Figure 4-2 also displays a good qualitative agreement with Hinze's theoretical prediction. Quantitatively, the results lower than the theoretical curve, but are closer in general to the theoretical results than the mean velocity results are. The results for $x/D_o > 20$ are within 0.02 U_o of the theoretical curve, with a maximum percentage difference of 60%.

Simo's results for the axial rms velocity distribution are extremely close to Hinze's theoretical curve, so there is excellent quantitative agreement between those earlier

results and the experimental results. In particular, the results which Simo obtained for $R_e = 26{,}000$ and the experimental results for $R_e = 27{,}900$ are very close, which is not surprising because the Reynolds numbers are so close.

Both of the axial velocity distributions which were obtained in the experiments serve to confirm the results which Simo obtained using the laser doppler system, and Hinze's theoretical predictions for the centerline velocity distributions in a round free gas jet. The excellent qualitative agreement suggests that Hinze's theoretical prediction is a good mathematical model of downstream jet velocities. The agreement between the experimental results and the theory is better for the higher Reynolds numbers of 20,000 and 26,540 or 27,900. This suggests that the validity of the theory decreases as the Reynolds number is decreased and the jet becomes less turbulent in nature.

5.2 Relative Turbulence Intensities

The relative turbulence intensities do not correlate well with Hinze's theoretical prediction. According to theory, the turbulence intensities should be constant at a level of $u'/U = 0.25$. Simo's turbulence intensities, while displaying a good deal of scatter, are between values of u'/U from 0.22 to 0.33. The experimental turbulence intensities rise in a nearly linear fashion for all Reynolds numbers, so there is no apparent correlation with the theory.

Because the theoretical prediction for turbulence intensity has been confirmed by a multitude of experiments, it appears that there is some degree of error in the experimental turbulence intensities which were obtained. During the experiment, the rms voltages which were obtained were nearly constant for all downstream distances, particularly for the lower Reynolds numbers of 10,000 and 15,000. In fact, these rms voltages should have been steadily decreasing, since the downstream rms velocities should be smaller in order to maintain the ratio of 0.25 for u'/U. This observation leads to the hypothesis that there was some degree of white noise present in the electronics of the measurement system which affected the hot-wire anemometer output

voltages. This assumption was confirmedf white noise present in the electronics of the measurement system which affected the hot-wire anemometer output voltages. This assumption was confirmed by the observation of white noise in the power spectra of the velocity waveforms at R_e = 20,000, which will be discussed in the next section. The white noise present in the measurement system resulted in inaccurate readings for the rms voltage, which in turn caused inaccurate rms velocity calculations. Thus, although the axial velocity profiles are correct, and a good confirmation of Hinze's theory and Simo's results, the turbulence intensities u'/U_o must be disregarded with respect to the earlier results due to the error present in the measurement system.

5.3 Power Spectra

The power spectra of the jet at R_e =20,000 display the expected decrease in density as the frequency of the turbulent fluctuations increases. For $x/D_o \leq 20$, the power spectra have large peaks all through the frequency spectrum, indicating the presence of significant high frequency turbulence. For x/D_o of 30 or greater, though, the power spectra fall off at high frequencies, indicating that the majority of the turbulent velocity fluctuations have low frequencies.

The power spectra exhibit a small white noise level as they fall off at high frequencies, reaching a final average value which is greater than zero. Although the amount of noise is not excessively large, it did have an effect on the rms velocity measurements. The high frequency noise in the electronics of the measurement system led to inaccurate rms voltage readings, which in turn caused inaccurate rms velocity calculations. This led to the large discrepancy between the theoretical prediction and the experimental results in the turbulence intensities.

Chapter 6

Conclusions

The hot-wire anemometer measurements were successful in confirming the axial mean and rms velocity profiles for an axisymmetric turbulent jet which were predicted by Hinze and found experimentally by Simo. There was very good qualitative agreement between the experimental results and those given by Hinze and Simo for the shape of the nondimensional axial velocity profile, particularly at higher Reynolds numbers. The experimental results were lower than Simo's results and Hinze's predictions by about 20% in most cases.

Due to the degree of white noise in the measurement system, the turbulence intensities which were found do not correlate well with either Simo's results or Hinze's theoretical prediction of $u'/U = 0.25$. The noise caused the rms voltage readings to be inaccurate, which in turn led to inaccurate values for the rms velocity. The experimental results demonstrate a nearly linear increase in turbulence intensity with nondimensional downstream distance. Since numerous previous experiments have confirmed the validity of Hinze's theoretical prediction, it must be assumed that the experimental results obtained in this case are inaccurate.

The power spectra of the downstream turbulent velocities for $R_e = 20{,}000$ exhibited the expected behavior for downstream distances of x/D_o of 30 or greater, since density decreased as the frequency increased. Closer to the nozzle, very significant high-frequency turbulence was observed. A small degree of white noise was observed as the power spectra fell off at high frequencies, which explains the discrepancy in

the turbulence intensities.

Bibliography

[1] Philip M. Gerhart and Richard J. Gross. *Fundamentals of Fluid Mechanics.* Addison-Wesley, Reading, MA, 1985.

[2] J.O. Hinze. *Turbulence.* McGraw-Hill Book Company, New York, 1975.

[3] John H. Lienhard. *A Heat Transfer Textbook.* Prentice-Hall, Englewood Cliffs, NJ, 1987.

[4] John A. Simo. *Turbulent Transport of Inertial Aerosols.* Massachusetts Institute of Technology, Cambridge, MA, 1991.

[5] H. Tennekes and J.L. Lumley. *A First Course In Turbulence.* The MIT Press, Cambridge, MA, 1972.